JOURNAL OF CATALYSIS 124, 109–115 (1990)

Active Sites in Oxide-Promoted Metal Catalysts: CO Chemisorption on AlO_x-Modified Ni(111)

YONG-BO ZHAO AND YIP-WAH CHUNG

Department of Materials Science and Engineering, and Center for Catalysis and Surface Science, Northwestern University, Evanston, Illinois 60208

Received December 5, 1989; revised February 5, 1990

CO chemisorption on both clean Ni(111) and AlO_x(x is between 0.5 and 1.1)-modified Ni(111) surfaces at 200 K has been studied by Auger electron spectroscopy (AES), thermal desorption spectroscopy (TDS), and high-resolution electron energy loss spectroscopy (HREELS). The AlO_x/Ni(111) specimen was prepared by evaporating Al onto the Ni surface and then oxidizing and reducing the specimen at 700 K. TDS results showed that the presence of surface AlO_x species suppresses CO chemisorption and that the suppression is almost a linear function of the AlO_x coverage. The most prominent CO desorption peak on Ni occurs at 415 K. This peak intensity decreases with increasing AlO_x coverage, indicating a site-blocking effect. An additional CO desorption peak at 300 K was found on the AlO_x-modified Ni surface. This 300 K peak intensity attains a maximum at some intermediate AlO_x coverage. HREELS results showed a new C–O stretching frequency of 1613 cm^{-1} for CO adsorbed on the AlO_x/Ni surface. The disappearance of this 1613-cm^{-1} energy loss peak upon heating the surface to 325 K suggests that both the 300 K TDS peak and the 1613-cm^{-1} energy loss peak represent the same adsorbed CO state, which is attributed to CO absorbed on AlO_x/Ni perimeter sites. Surface morphology of the oxide islands and significance of the perimeter sites are discussed.

INTRODUCTION

Since the detailed report by Tauster *et al.* of strong metal–support interaction (SMSI) in several systems (*1*), the cause of this interesting effect has been an area of great activity in the surface science–catalysis community. SMSI is characterized by the loss of H_2 and CO chemisorption capability of the supported metals (*1–6*) and drastic activity and selectivity changes in certain chemical reactions (*7–12*). The typical condition to generate SMSI is reduction in H_2 at 773 K, and it is now well recognized that under such condition the support migrates to the metal surface in a reduced state (*4, 6, 13, 14*).

Whether or not a catalyst would exhibit SMSI behavior is found to be strongly related to the reducibility of the supporting oxide (*2*). SMSI effects depend on reduction conditions. In the case of Al_2O_3 as a support, it was found that after reduction at 773 K no SMSI effects were observed (*2*). After increasing the reduction temperature from 773 to 973 K, however, the amount of H_2 adsorbed by Pt/Al_2O_3 decreased about 60% (*15*). After 18-h reduction at 1273 K, Al was detected at the surface of Pt/Al_2O_3 (*16*). This indicates that although under normal SMSI conditions, i.e., reduction at 773 K, Al_2O_3 as a support does not exhibit significant SMSI effects, it might be possible to induce SMSI under more severe reduction conditions.

Previous work in this lab showed that upon deposition of TiO_x and MnO_x on Ni(111), a new CO adsorption state was produced (*3, 6*). This adsorption state was attributed to CO adsorbed at metal–oxide perimeter sites, which are considered to be the active sites in CO hydrogenation reactions. For Al_2O_3-supported metal catalysts, it is rather difficult to reduce the catalysts so that a controlled amount of reduced AlO_x species would migrate to the surface. It would be even more difficult for SiO_2-supported metal catalysts. Using a metal/

0021-9517/90 $3.00

oxide evaporator, however, one can put submonolayer amounts of AlO_x on the metal surface to simulate the SMSI state and study surface oxide effects. It is interesting to find out what the effects are when an oxide like Al_2O_3, which is normally considered a non-SMSI support (*2*), is present on the catalyst surface.

The present study, therefore, was conducted to prepare AlO_x-modified Ni(111) model catalysts, to investigate the effects of this oxide on CO chemisorption, and then to establish a correlation between CO chemisorption and surface morphology of the oxide. In particular, experiments were carried out to characterize the surface composition, CO adsorption states, and the amount of CO adsorbed on the surface under different conditions.

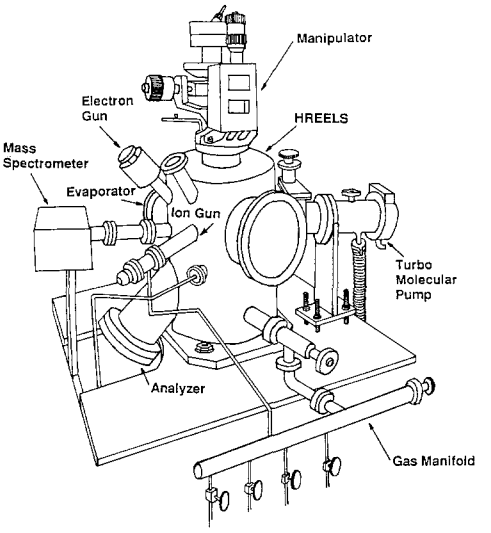

FIG. 1. Schematic diagram of the experimental setup.

EXPERIMENTAL

All experiments were carried out in an ultrahigh vacuum (UHV) chamber which is equipped with an Auger electron spectrometer, a metal/oxide evaporator, an ion gun, a quadrupole mass spectrometer, and a high-resolution electron energy loss spectrometer. A schematic diagram of this setup is shown in Fig. 1. The specimen was mounted on a manipulator that can be moved to different positions for surface preparation and data acquisition. The specimen could be cooled to 150 K or heated at up to 7 K/s to 900 K. The surface temperature was monitored with a W/5%Re–W26%Re thermocoupled spotwelded to the specimen surface.

The specimen used in these experiments was a Ni(111) single crystal disk about 1 cm^2 in surface area and 1 mm in thickness. The surface was cleaned first by Ar ion sputtering and annealing at 700 K under UHV for a few cycles to remove bulk impurities, followed by one or two oxidation–reduction cycles to remove surface impurities. The evaporation source consisted of thin metallic Al wires wrapped on a W filament. During evaporation, the filament was heated to about 940 K with the Ni surface held at room temperature. The amount of Al deposited was determined with a quartz crystal thickness monitor which has a resolution of 1/4 monolayer for Al. The specimen was oxidized under 1×10^{-5} Torr oxygen at room temperature for 60 min and then reduced under 2×10^{-6} Torr hydrogen at 773 K for 15 min. From our experience, such a reduction treatment will produce an unoxidized and smooth nickel surface. The oxygen-to-aluminum ratio was calibrated using 35 eV (Al) and 503 eV (O) Auger peak intensities. AES data showed that the oxygen-to-aluminum ratio after reduction was between 0.5 and 1.1. Each time after a surface was prepared, it was cooled to 200 K for CO exposure. Carbon monoxide (99.99% purity) was purified by passing it through a liquid-nitrogen-cooled stainless-steel thin tubing to remove residual water and metal carbonyls before it was introduced into the chamber. In all experiments, the CO exposure was fixed at 300 Langmuirs (L). AES was performed at a primary electron energy of 1600 eV using a Comstock electron analyzer in sector-sweeping mode and with a modulation amplitude of 2 eV. The surface composition

was characterized by four major Auger peaks at 272 eV (C), 503 eV (O), 35 eV (Al), and 848 eV (Ni). Thermal desorption was performed by ramping the temperature of the Ni specimen from 200 to 700 K at 7 K/s. In high-resolution electron energy loss spectroscopy (HREELS) studies, the electron beam was set at 2 eV primary energy (uncorrected for work function difference), and the surface was maintained at 200 K unless indicated otherwise. All energy loss spectra were taken with elastic peak resolution better than 88 cm^{-1}. The surface was cleaned and reprepared between thermal desorption or HREELS experiments.

RESULTS

Several Ni(111) surfaces were prepared with different surface coverages of AlO_x. Our quartz thickness monitor showed that the amount of aluminum deposited varied from 0 to 4.2×10^{15} atoms/cm^2, the latter corresponding to an average oxide coverage of about 2.8 monolayers. Results of CO thermal desorption from these surfaces are shown in Fig. 2. From a clean Ni(111) surface, the most prominent CO desorption peak is located at 415 K. With increasing amount of AlO_x on Ni, the 415 K peak becomes weaker. At the same time, a new feature at 300 K grows with increasing AlO_x coverage, reaches a maximum at an intermediate AlO_x coverage, and then decreases until it vanishes at a coverage of 4.2×10^{15} aluminum atoms/cm^2 or 2.8 monolayers of oxide. The fact that complete suppression of CO chemisorption occurred at an average oxide coverge of 2.8 monolayers instead of one monolayer indicates three-dimensional island formation for the oxide. In Fig. 3, areas under these two peaks are plotted as a function of the average surface AlO_x coverage. The 415 K peak decreases in intensity almost linearly with increasing AlO_x coverage. The new 300 K feature can be interpreted readily in terms of CO adsorption at or near the perimeter of oxide islands on the Ni(111) surface. At low oxide coverage, the concentration of such perimeter sites is low. At sufficiently high oxide coverage, the nickel surface is completely covered, leading again to low perimeter site concentration. Therefore, at some optimum oxide coverage, the perimeter site concentration attains a maximum. Clearly, the optimum oxide coverage and the actual site concentration must depend on the average size of these oxide islands. It is interesting to note that a similar feature was observed for CO adsorbed on MnO_x-modified Ni(111) (*6*).

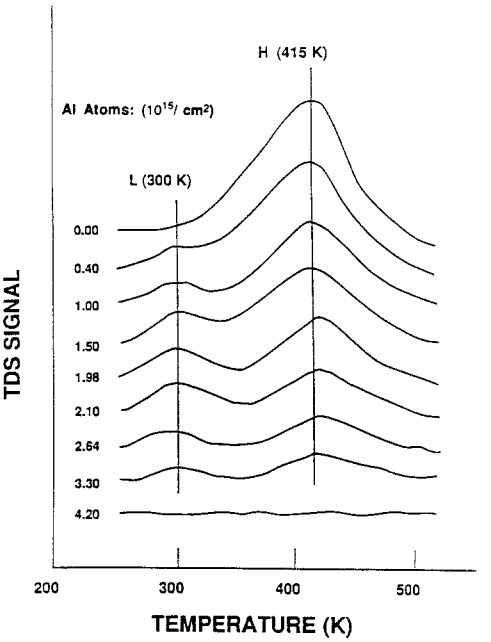

FIG. 2. Series of thermal desorption spectra of CO from AlO_x-modified Ni(111) surface with different AlO_x coverages as indicated by the number of Al atoms on Ni varying from 0 to $4.2 \times 10^{15}/cm^2$. CO chemisorption was made by introducing 300 liters CO into the UHV chamber while the specimen was at 200 K. During thermal desorption, the surface was heated at about 7 K/s.

Figure 4a shows the electron energy loss spectrum of CO adsorbed on a clean Ni(111) surface at 200 K. We were not able to obtain any meaningful data in the loss region corresponding to Ni–C and Al–O stretch. This is apparently due to the rough topography of the AlO_x-modified Ni(111) surface, resulting in a long elastic peak tail

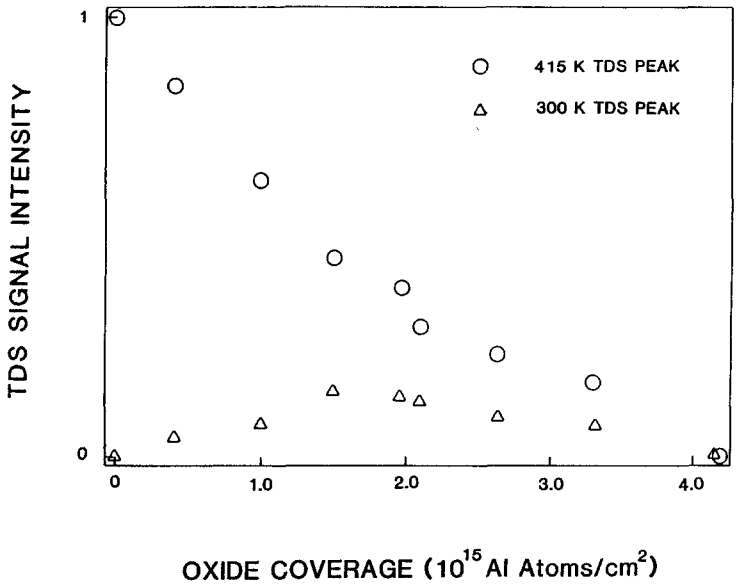

FIG. 3. Variation of CO thermal desorption peak intensity as a function of oxide coverage.

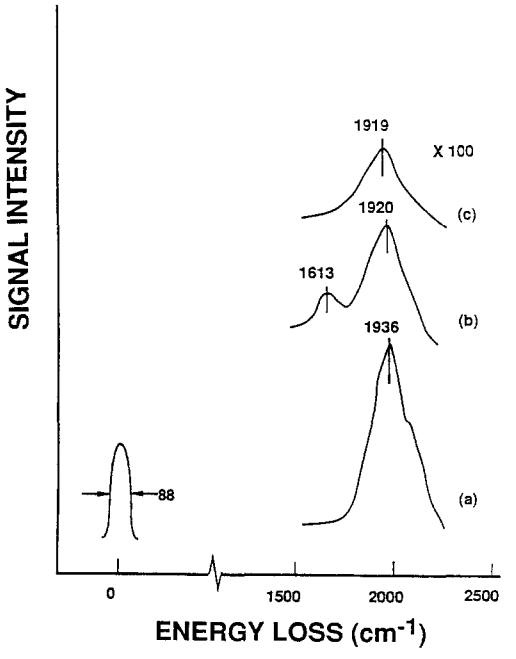

FIG. 4. High-resolution electron energy loss spectrum of: (a) Ni(111) surface exposed to 300 liters CO at 200 K; (b) AlO_x-modified Ni(111) surface exposed to 300 liter CO at 200 K; (c) surface in Fig. 4b after being heated to 325 K for 5 min.

and obscuring both the Ni–C and Al–O loss peaks. The major peak at 1936 cm^{-1} (carbon–oxygen stretching due to bridge-bonded CO on Ni) and a small shoulder around 2033 cm^{-1} (carbon–oxygen stretching due to ontop-bonded CO on Ni) are well documented in the literature (*17–19*). Figure 4b shows the loss spectrum due to CO adsorbed on a Ni(111) surface partially covered with AlO_x species. A small new peak at 1613 cm^{-1} is observed here. A similar feature was observed previously on MnO_x/Ni(111) (*6*). The interpretation made then was that the CO molecule adsorbed on the MnO_x/Ni perimeter site is activated on the oxygen end by surface MnO_x, thereby weakening the C–O bond and lowering the C–O stretching frequency. A similar interpretation can be applied to the AlO_x/Ni(111) system. That is, the 1613-cm^{-1} energy loss peak, which is related to the C–O stretching, and the 305 K thermal desorption peak, which is related to the CO–surface bonding, are from the same CO adsorption state, i.e., CO adsorbed at or near the AlO_x/Ni perimeter sites. Figure 4c shows the energy loss spectrum which was

taken at room temperature after the surface shown in Fig. 4b had been heated to 325 K for 5 min. The 1613-cm^{-1} peak disappeared immediately after the surface was heated to 325 K.

DISCUSSION

In early studies of SMSI, the typical method to generate SMSI effects was to reduce the catalysts at elevated temperatures. As mentioned before, the typical reduction temperature is around 773 K. For these SMSI-active supports (*2*), it usually takes between a few minutes and a few hours to create significant effects. Now it is well known that such a reduction results in a partial coverage of the metal surface with reduced support material. It has been recognized that whether or not a catalyst will show SMSI behavior is strongly related to the oxide used as support material. The most commonly studied support is TiO_2, for it is very easy to generate SMSI effects. On the other hand, support like SiO_2 is considered to be inert to SMSI. This suggests that under typical reduction conditions to induce SMSI, either the migration rate of the support is too low to produce any observable amount of surface oxide or the oxide is so stable that no significant interaction between the metal and the support takes place.

Although considered a very stable support (*2*), Al_2O_3 is not completely inert to SMSI. Weller and Montagna reported that pure Al_2O_3 is not completely inactive to dry H_2 at temperatures of about 773 K (*20*). They interpreted the observed H_2 consumption as being due to a reduction of alumina to an aluminum suboxide. After reduction at temperatures below 773 K, Al_2O_3-supported iridium catalysts did not show SMSI behavior (*2*). But after reduction at temperatures up to 973 K, it was found that a large fraction of the Pt in Pt/Al_2O_3 became "inaccessible" to hydrogen chemisorption (*21, 22*). Den Otter and Dautzenberg suggested that the presence of platinum on the Al_2O_3 increases the reduction rate. They concluded that the inability of Pt on Al_2O_3 to chemisorb H_2 after high-temperature reduction was due to a Pt-assisted reduction of the Al_2O_3 support, leading to the formation of a Pt/Al alloy (*22*). In another study of the 2000-Å Pt/Al_2O_3 system, results showed that an 18-h reduction at 1273 K can cause the support to be partially reduced (oxygen-to-aluminum ratio near 1) and to be detected on the surface (*16*). The results presented in our study show that at 773 K a small amount of Al_2O_3 (less than three monolayers) is readily reduced to a suboxide with an oxygen-to-aluminum ratio between 0.5 and 1.1 (*23*).

The thermal desorption data in Fig. 3 show that the suppression of CO chemisorption is almost a linear function of the surface AlO_x coverage. Such a linear relation between chemisorption suppression and oxide coverage was also found in MnO_x/Ni(111) model catalysts (*6*) and TiO_x/Pt (*5*), and it indicates that the suppression is caused mainly by physical blockage of metal surface sites. The 2.8 monolayer oxide coverage at which complete suppression of CO on AlO_x/Ni(111) occurs suggests that AlO_x does not spread evenly over the surface, but rather forms three-dimensional islands. This is in agreement with the observation by Ko and Gorte (*24*) that relatively large quantities of oxide were necessary to prevent the adsorption.

Results of CO chemisorption studies from both the AlO_x/Ni(111) and MnO_x/Ni(111) model catalyst show that new chemisorption sites are created when a nickel surface is modified by reduced oxides. Although the exact configuration of these new sites is unknown, the fact that their presence requires the surface to be partially covered by reduced oxides strongly suggests the involvement of the metal as well as reduced oxide sites. At this moment, we favor a model similar to that proposed by Vannice and Sudhaker and Sachtler and coworkers (*25, 26*). In this model, taking AlO_x/Ni(111) as an example, each new site consists of both AlO_x at the oxide island

perimeter and Ni in the immediate vicinity, with the CO adsorbed on the Ni and the oxygen end of the CO activated by the AlO_x species. TDS and HREELS results reveal that CO in this adsorption state has weaker C–Ni and C–O bonds, as indicated by the lower thermal desorption temperature and lower C–O stretching frequency. We believe that under these conditions, CO dissociation as well as the desorption process involved in the CO–H_2 reaction would become easier and faster. In this way, the reduced oxide clusters act as promoters to enhance the CO hydrogenation activity over metal surfaces (such as Ni, Pd, Pt) where CO dissociation is an important rate-determining step (*9, 27–31*). It has been found that after high-temperature reduction, Al_2O_3-supported metal catalysts showed a methanation activity more than 10 times higher than that of SiO_2-supported catalysts (*9, 10, 32*), and the difference in activity was found to be related to the difference in CO dissociation rate (*32, 33*). Such perimeter-site-related CO hydrogenation activity has also been observed recently on TiO_x/Rh catalysts (*34*). These observations are consistent with our results and support the model proposed here.

It is somewhat surprising that the low-frequency C–O stretch is so similar in energy for AlO_x- and MnO_x-modified Ni(111), given the fact that Al and Mn are chemically very different. One explanation is as follows. The lowering of the C–O stretch frequency depends on the oxophilicity of the metal oxide islands, which in turn depends on how far the metal oxide is reduced. Since the reduction treatment is the same for MnO_x and AlO_x, one can argue that the effect on C–O stretch should be approximately the same. Of course, if the reduction treatment is severe enough to fully reduce the metal oxide, the oxophilicity simply depends on the metal itself, at which point one would expect to see dependence of the C–O stretch on the metal.

CO chemisorption also indicates that at the optimum oxide coverage, the concentration of these perimeter sides is only about 10% of the available metal surface atoms. This does not contradict the proposed model that these perimeter sites are the active sites in CO hydrogenation because it is found that the number of active sites in a CO hydrogenation reaction is a very small fraction of the total metal surface sites (*8, 29, 35*). It has also been found that once the metal/reduced oxide ensembles are formed, they cannot easily be fully oxidized (*36*). Therefore, the SMSI effects are quite durable under CO hydrogenation reaction conditions (*37*). This indicates that the chemistry at these sites is not due to a simple superposition of the metal and the reduced oxide.

CONCLUSIONS

(1) CO chemisorption has been performed on Ni(111) and AlO_x-modified Ni(111) surfaces at 200 K. From thermal desorption and energy loss spectra, it is found that the presence of surface AlO_x species suppresses CO chemisorption and that the suppression is almost a linear function of the oxide coverage.

(2) For CO adsorbed on AlO_x-modified Ni(111) surfaces, additional features of both a lower temperature thermal desorption peak at 300 K and a lower C–O stretching frequency peak at 1613 cm^{-1} are observed. The 1613-cm^{-1} energy loss peak disappears when the surface is heated to 325 K, which indicates that these two features come from the same new CO adsorption state.

(3) The above results suggest that the 300 K TDS peak and the 1613-cm^{-1} energy loss peak are due to CO adsorption at or near the surface AlO_x/Ni perimeter sites. Such an adsorption state is believed to be important in enhancing the CO hydrogenation activity in an SMSI system.

ACKNOWLEDGMENTS

Acknowledgment is made to the Donors of the Petroleum Research Fund, administered by the American Chemical Society, for support of this research. We

thank Professors Sachtler and Ichikawa for many illuminating discussions.

REFERENCES

1. Tauster, S. J., Fung, S. C., and Garten, R. L., *J. Amer. Chem. Soc.* **100,** 170 (1978).
2. Tauster, S. J., and Fung, S. C., *J. Catal.* **55,** 29 (1978).
3. Takatani, S., and Chung, Y. W., *J. Catal.* **90,** 75 (1984).
4. Takatani, S., and Chung, Y. W., *Appl. Surf. Sci.* **19,** 341 (1984).
5. Dwyer, D. J., Cameron, S. D., and Gland, J., *Surf. Sci.* **195,** 430 (1985).
6. Zhao, Y. B., and Chung, Y. W., *J. Catal.* **106,** 369 (1987).
7. Vannice, M. A., and Garten, R. L., *J. Catal.* **56,** 29 (1979).
8. Vannice, M. A., Wang, S. Y., and Moon, S. H., *J. Catal.* **71,** 152 (1981).
9. Wang, S. Y., Moon, S. H., and Vannice, M. A., *J. Catal.* **71,** 167 (1981).
10. Vannice, M. A., Twu, C. C., and Moon, S. H., *J. Catal.* **79,** 70 (1983).
11. Resasco, D. E., and Haller, G. L., *J. Catal.* **82,** 279 (1983).
12. Chung, Y. W., Xiong, G. X., and Kao, C. C., *J. Catal.* **85,** 237 (1984).
13. Santos, J., Phillips, J., and Dumesic, J. A., *J. Catal.* **83,** 168 (1983).
14. Jiang, X. Z., Hayden, T. F., and Dumesic, J. A., *J. Catal.* **83,** 168 (1983).
15. Baker, R. T., Prestridge, E. B., and McVicker, G. B., *J. Catal.* **89,** 422 (1984).
16. Cairns, J. A., Baglin, E. E., Clark, G. J., and Ziegler, J. F., *J. Catal.* **83,** 301 (1983).
17. Erley, W., Wagner, H., and Ibach, H., *Surf. Sci.* **80,** 612 (1979).
18. Erley, W., Ibach, H., Lehwald, S., and Wagner, H., *Surf. Sci.* **83,** 585 (1979).
19. Campuzano, J. C., and Greenler, R. G., *Surf. Sci.* **83,** 301 (1979).
20. Weller, S. W., and Montagna, A. A., *J. Catal.* **21,** 303 (1971).
21. Dautzenberg, F. M., and Wolters, H. B. M., *J. Catal.* **51,** 26 (1978).
22. Den Otter, G. J., and Dautzenberg F. M., *J. Catal.* **53,** 116 (1978).
23. Zhao, Y. B., Lin, T. S., and Chung, Y. W., *Mater. Res. Soc. Symp. Proc.* **111,** 435 (1988).
24. Ko, C. S., and Gorte R. J., *Surf. Sci.* **155,** 296 (1985).
25. Vannice, M. A., and Sudhakar, C., *J. Phys. Chem.* **88,** 2429 (1984).
26. Sachtler, W. M. H., Shriver, D. F., Hollenberg, W. B., and Lang, A. F., *J. Catal.* **92,** 429 (1985).
27. Sughrue, E. L., and Bartholomew, C. H., *Appl. Catal.* **2,** 239 (1982).
28. Van Meerten, R. Z. C., Vollenbrock, J. G., de Groon, M. H. J. M., Van Nisserlrooy, P. F. M. T., and Coenen, J. W. E., *Appl. Catal.* **3,** 29 (1982).
29. Vannice, M. A., and Twu, C. C., *J. Catal.* **82,** 213 (1983).
30. Mori, T., Masuda, H., Imai, H., Miyamoto, A., Hasebe, R., and Murakami, Y., *J. Phys. Chem.* **87,** 3648 (1983).
31. Vannice, M. A., Leong, T., and Sudhakar, C., *Prepr. Amer. Chem Soc. Div. Pet Chem.* **29,** 558 (1984).
32. Bartholomew, C. H., and Vance, C. K., *J. Catal.* **91,** 78 (1985).
33. Erdohelyi, A., and Solymosi, F., *J. Catal.* **84,** 446 (1983).
34. Levin, M. E., Salmeron, M., Bell, A. T., and Somorjai, G. A., *J. Catal.* **106,** 401 (1987).
35. Burch, R., and Flambard, A. R., *J. Catal.* **78,** 389 (1982).
36. Greenlief, C. M., White, J. M., Ko, C. S., and Gorte, R. J., *J. Phys. Chem.* **89,** 5025 (1985).
37. Dwyer, D. J., Robbins, J. L., Cameron, S. D., Dudash, N., and Hardenberg, J., *in* "Strong Metal–Support Interactions," *ACS Symp. Ser.* **298,** 21 (1986).